Optimal Power Capturing of Multi-MW Wind Generation System

KONG YIGANG, WANG ZHIXIN
Department of Electrical Engineering
Shanghai Jiao Tong University
Minhang District, Shanghai 200240
CHINA
kongyg@sjtu.edu.cn wangzxin@sjtu.edu.cn

Abstract: - Recently, an increasing number of multi-MW (1MW and up) wind generation systems are being developed and variable speed-variable pitch (VS-VP) control technology is usually adopted to improve the fast response speed and obtain the optimal energy, which means to obtain the maximum power at low wind speed and the rated power at high wind speed. However, the power generated by wind turbine changes rapidly for the continuous fluctuation of wind speed and direction, and wind energy conversion systems are of strong nonlinear characteristics for many uncertain factors and external disturbances. Based on modeling and analyzing of the doubly-fed induction generator (DFIG) and the hydraulic variable pitch mechanism (HVPM), this paper presents an adaptive fuzzy proportional integral derivative (AFPID) control strategy to capture optimal power. Simulation results show that the controller can improve the wind turbine performance than conventional PID controller.

Key-Words: - Doubly-fed induction generator, Hydraulic variable pitch mechanism, Optimal, Adaptive fuzzy proportional integral derivative, Variable speed-variable pitch, Wind turbine

1 Introduction

Compared with fossil fuel and nuclear power generation, wind power is cost competitive, environmentally clean and safe renewable power sources, and is being paid more attention recently [1]. An actual turbine cannot extract more than 59.3 percent of the air kinetic energy according to Betz theory [2]. In practice, this factor is less because of mechanical imperfections, but we take all efforts to obtain the maximum energy by adopting various methods.

On the other hand, in a renewable energy system, power quality and reliability are two most vulnerable issues. The ordinary linear constant gain controller will cause overshoot or even loss of system stability. At the same time the adaptive control method is not applicable in this case due to the complexity of the algorithm and the fast response characteristic of the multi-MW VS-VP wind turbine. When the wind speed range varies from the cut-in wind speed to the rated wind speed, variable speed control method is adopted. Objectives for variable speed control system are summarized by the following general goals: to regulate and smooth the generated power, to maximize the energy capture, to alleviate the transient loads. When the wind speed range varies from the rated wind speed to the cut-out wind speed, variable pitch control method is adopted. Objectives for variable pitch control are similar to the variable speed ones but only can be match a rotational power by regulating pitch angle [3].

The conventional PID control has been used in industry for many years because of its simpler structure and good robust performance. However, the resulting control system performance fully depends on the tuning of its parameters. It has been a problem to tune properly these parameters because wind generation system is often burdened with problems such as high order, time delays, and nonlinearities [4, 5]. The fuzzy control can overcome uncertain parameters and unknown models of nonlinear systems and has a fast response characteristic. The ideas of full order feedback and membership function are used in the design of the controller, which can be called adaptive fuzzy PID controller (AFPIDC).This paper describes a 1.5 MW VS-VP wind generation system with the DFIG and the HVPM where an AFPIDC has been used extensively to optimize the power output and enhance the system performance [6-8].

2 Wind Turbine System

A simplified VS-VP wind generation system is show in Fig.1, which can be divided into seven parts briefly, such as blade, gear box, DFIG, power grid, variable pitch mechanism, converter and controller.

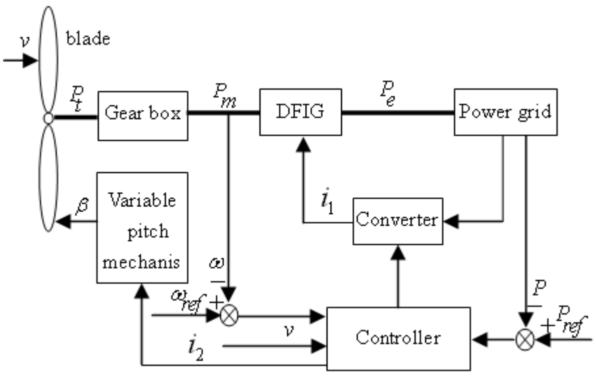

Fig.1 A simplified VS-VP wind generation system

2.1 Wind Turbine

The main objective of using a VS-VP control strategy is to improve the fast response speed and obtain the optimal energy. The aerodynamic power captured by the wind turbine is calculated by nonlinear expression

$$P_t = \frac{1}{2}\rho\pi R^2 C_p(\lambda,\beta)v^3 \tag{1}$$

The wind turbine torque is given by

$$T_t = \frac{1}{2}\rho\pi R^3 C_q(\lambda,\beta)v^2 \tag{2}$$

There is an expression between the power coefficient $C_p(\lambda,\beta)$ and the torque coefficient $C_q(\lambda,\beta)$

$$C_p(\lambda,\beta) = \lambda C_q(\lambda,\beta) \tag{3}$$

where $\lambda = \omega_t R / v$ is the tip speed ratio, ω_t is the turbine angular velocity (rad/s), v is the wind speed (m/s), ρ is the air density (kg/m^3), R is the rotor radius (m) and β is the pitch angle (°). $C_p(\lambda,\beta)$ and $C_q(\lambda,\beta)$ are two nonlinear function of λ and β. At $\lambda = 10$, $\beta = 0$, the optimum power coefficient can be obtained, and its characteristic is shown in Fig.2.

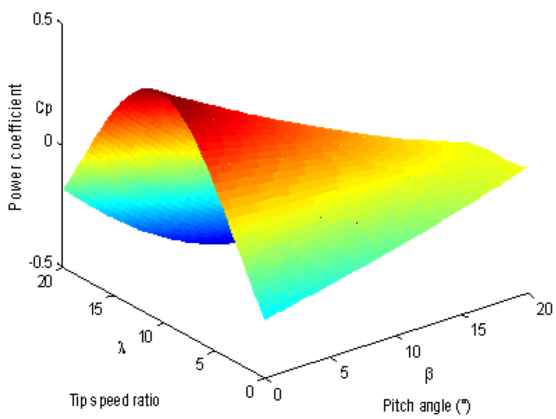

Fig.2 Coefficient curve of wind turbine power

2.2 Gear Box

In the mechanical model, the torque of high speed shaft T_m is calculated by the expression

$$J_t \frac{\mathrm{d}\omega_t}{\mathrm{d}t} = T_t - n_t T_m \tag{4}$$

where T_t is the wind turbine torque (N·m), J_t is wind turbine rotor inertia (kg·m^2), n_t is the gear drive train ratio. The gear drive train is considered because it has the most significant influence on the power fluctuations.

2.3 Doubly-fed Induction Generator

DFIG is adopted mostly in a multi-MW VS-VP wind turbine, and its characteristic is that the stator windings are directly connected to the three-phase grid and the rotor windings are connected to a frequency converter, which control the rotor current's phase and magnitude and are therefore used for active power and reactive power control. Using the electric motor convention and adopting the $d-q$ reference frame, the following equation for DFIG model can be achieved

$$\begin{cases} u_{ds} = R_s i_{1ds} - \omega_s \psi_{qs} + \dfrac{\mathrm{d}\psi_{ds}}{\mathrm{d}t} \\ u_{qs} = R_s i_{1qs} + \omega_s \psi_{ds} + \dfrac{\mathrm{d}\psi_{qs}}{\mathrm{d}t} \\ u_{dr} = R_r i_{1dr} - (\omega_s - \omega_r)\psi_{qr} + \dfrac{\mathrm{d}\psi_{dr}}{\mathrm{d}t} \\ u_{qr} = R_r i_{1qr} + (\omega_s - \omega_r)\psi_{dr} + \dfrac{\mathrm{d}\psi_{qr}}{\mathrm{d}t} \\ \psi_{ds} = L_{ls} i_{1ds} + L_m(i_{1ds} + i_{1dr}) \\ \psi_{qs} = L_{ls} i_{1qs} + L_m(i_{1qs} + i_{1qr}) \\ \psi_{dr} = L_{lr} i_{1dr} + L_m(i_{1ds} + i_{1dr}) \\ \psi_{qr} = L_{lr} i_{1qr} + L_m(i_{1qs} + i_{1qr}) \end{cases} \tag{5}$$

where subscripts d and q denote the direct and quadrature axes of the reference frame, the $d-q$ reference frame is rotating at synchronous speed with the q axis 90° ahead of the d axis [9, 10]. Subscripts s and r denote stator and rotor variables. u is the voltage (V), R_s and R_r are the stator and rotor resistances (Ω), i_1 is the current (A), ω_s is the stator electrical angular velocity (rad/s), ω_r is the rotor electrical angular velocity (rad/s), and ψ is the flux linkage (Wb), L_{ls} is the flux leakage of the stator windings (H), L_{lr} is the flux leakage of the rotor windings (H), and L_m is the mutual (magnetizing) inductance between the stator and the rotor windings (H).

Eliminating flux linkage ψ from Eq.(5), the DFIG model can be expressed

$$\begin{bmatrix} \frac{\mathrm{d}i_{1ds}}{\mathrm{d}t} \\ \frac{\mathrm{d}i_{1qs}}{\mathrm{d}t} \\ \frac{\mathrm{d}i_{1dr}}{\mathrm{d}t} \\ \frac{\mathrm{d}i_{1qr}}{\mathrm{d}t} \end{bmatrix} = k \begin{bmatrix} R_sL_{lr} & -[\omega_sL_{ls}L_{lr}-(\omega_s-\omega_r)L_m^2] & -R_rL_m & -\omega_rL_{lr}L_m \\ [\omega_sL_{ls}L_{lr}-(\omega_s-\omega_r)L_m^2] & R_sL_{lr} & \omega_rL_{lr}L_m & -R_rL_m \\ -R_sL_m & \omega_rL_{ls}L_m & R_rL_{ls} & [\omega_sL_m^2-(\omega_s-\omega_r)L_{ls}L_{lr}] \\ -\omega_rL_{ls}L_m & -R_sL_m & -[\omega_sL_m^2-(\omega_s-\omega_r)L_{ls}L_{lr}] & R_rL_{ls} \end{bmatrix} \begin{bmatrix} i_{1ds} \\ i_{1qs} \\ i_{1dr} \\ i_{1qr} \end{bmatrix} + k \begin{bmatrix} -L_{lr} & 0 & L_m & 0 \\ 0 & -L_{lr} & 0 & L_m \\ L_m & 0 & -L_{ls} & 0 \\ 0 & L_m & 0 & -L_{ls} \end{bmatrix} \begin{bmatrix} u_{ds} \\ u_{qs} \\ u_{dr} \\ u_{qr} \end{bmatrix} \quad (6)$$

where $k = 1/(L_m^2 - L_{ls}L_{lr})$. The relation between the electrical torque T_e and the mechanical torque T_m is shown below

$$J_\mathrm{g}\frac{\mathrm{d}\omega_\mathrm{g}}{\mathrm{d}t} = T_\mathrm{m} - T_\mathrm{e} \quad (7)$$

where J_g is the DFIG inertia (kg·m^2), ω_g is the DFIG angular velocity (rad/s).

2.4 Variable Pitch Mechanism

HVPM is a hydraulic valve-controlled cylinder system in this study. Fig.3 shows the schematic of a simplified electro-hydraulic proportional pitch-controlled system used in many types of wind turbine plant.

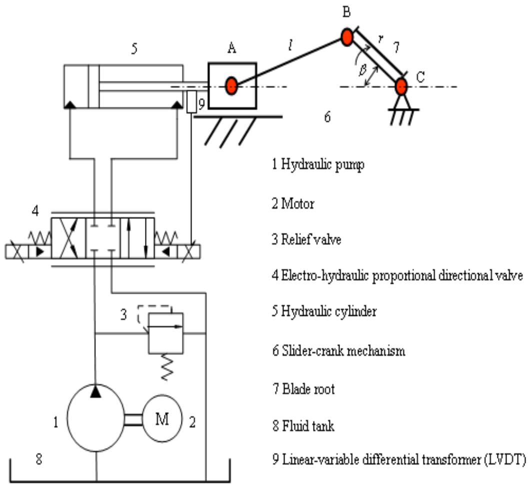

Fig.3 Schematic of a simplified HVPM

In the real pitch-regulated wind turbine, the blade is linked to the hydraulic cylinder by slider-crank mechanism. When the motor starts to work, the flow from the pump enters into the cylinder and forces the piston to move leftward or rightward according to the control signal. The change amount of the pitch angle is proportional to the cylinder motion, which is controlled accurately by the electro-hydraulic proportional valve. When the cylinder piston arrives at the leftmost side, the pitch angle is 0°. When the cylinder piston arrives at the rightmost side, the pitch angle is 90°. The displacement of the piston is measured by the linear-variable differential transformer (LVDT) which is then compared with the desired position and it is this error signal that is used as the feedback signal in the variable pitch control system.

Following the principles of electromagnetic induction, mechanical dynamics and fluid power behaviour, the governing equations can be developed for the components [11]. For the electromagnetic force in the electro-hydraulic proportional valve, the value is obtained as

$$F_i = K_i \cdot i_2 = K_{sf}x_v \quad (8)$$

The control current signal becomes

$$i_2 = \frac{K_{sf}}{K_i}x_v = K_bx_v \quad (9)$$

where i_2 is the control current of the electro-hydraulic proportional valve (mA), K_i is the pressure-current amplification factor of the electro-hydraulic proportional valve (N/mA), K_{sf} is the spring coefficient of the electro-hydraulic proportional valve (N/mm), x_v is the displacement of the electro-hydraulic proportional valve (mm), K_b is the combined coefficient (mA/mm).

The flow equation in the electro-hydraulic proportional valve can be given

$$Q_l = K_q x_v - K_c p_c \quad (10)$$

where Q_l is the flow of the electro-hydraulic proportional valve (l/s), p_c is the load pressure (Pa), K_q is the flow amplification gain of the electro-hydraulic proportional valve (m^2/s), K_c is the flow-pressure amplification gain of the electro-hydraulic proportional valve (l/N).

The flow equation in the cylinder can be achieved as follows:

$$Q_L = A_c \frac{dy}{dt} + \frac{V_c}{4\beta_e}\frac{dp_c}{dt} + C_l p_c \quad (11)$$

Eq.(11) can be written via Laplace transform:

$$Q_L = A_c sy + \frac{V_c}{4\beta_e} sp_c + C_l p_c \quad (12)$$

where s is the variable of Laplace transform, A_c is the area of the cylinder in non-rod chamber (mm^2), β_e is the effective bulk modulus (N/m^2), V_c is the total volume of the cylinder (mm^3), C_l is the coefficient of leakage.

Neglecting the compressibility of the oil, the motion equation of the cylinder can be represented in Eq.(13)

$$P_c A_c = M\frac{d^2 y}{dt^2} + B_c \frac{dy}{dt} + Ky + F_L \quad (13)$$

Eq.(13) can be written via Laplace transform:

$$P_c A_c = Ms^2 y + B_c sy + Ky + F_L \quad (14)$$

where y is the displacement of the cylinder (mm), M is the equivalent mass of the cylinder and the load (kg), B_c is the resistant coefficient of the cylinder, K is the spring coefficient of the cylinder (N/mm), F_L is the external disturbance (N).

In fact, neglecting the compressibility of the oil, the external disturbance F_L and the resistant coefficient of the cylinder B_c, combining Eq.(9), Eq.(12) and Eq.(14), eliminating middle variable, the open-loop transfer function between the input i_2 and the output y can be expressed

$$G_o(s) = \frac{Y(s)}{I_2(s)} = \frac{K_q}{A_c}\cdot\frac{1}{K_b}\cdot\frac{K_s}{s(\frac{s^2}{\omega_h^2} + \frac{2\xi_h}{\omega_h}s + 1)}$$
$$= \frac{K_e}{s(\frac{s^2}{\omega_h^2} + \frac{2\xi_h}{\omega_h}s + 1)} \quad (15)$$

where: K_s is the gain of the linear-variable differential transformer (mA/mm), $\omega_h = \sqrt{\frac{4\beta_e A_c^2}{V_c M}}$ is the natural frequency of the hydraulic system, $\xi_h = \frac{K_c}{A_c}\sqrt{\frac{\beta_e M}{V_c}}$ is the damping ratio of the hydraulic system, $K_d = \frac{K_q}{A_c}\cdot\frac{1}{K_b}$, $K_e = \frac{K_q}{A_c}\cdot\frac{K_s}{K_b}$ are the combined coefficents.

The closed-loop transfer function between the input i_2 and the output y can be represented as

$$G(s) = \frac{Y(s)}{I_2(s)} = \frac{\dfrac{K_d}{s(\frac{s^2}{\omega_h^2} + \frac{2\xi_h}{\omega_h}s + 1)}}{1 + \dfrac{K_d K_s}{s(\frac{s^2}{\omega_h^2} + \frac{2\xi_h}{\omega_h}s + 1)}}$$
$$= \frac{K_d}{s\left(\frac{s^2}{\omega_h^2} + \frac{2\xi_h}{\omega_h} + 1\right) + K_e} \quad (16)$$

It can be seen that the HVPM is a 3rd order model from Eq.(16). Because the natural frequency of the HVPM is far greater than that of the wind turbine, Eq.(16) can be simplified by a 1st order model as follows:

$$G(s) = \frac{Y(s)}{I_2(s)} = \frac{K_d}{s + K_d K_s} = \frac{K_d}{s + K_e} \quad (17)$$

The relationship for the displacement of slider y (namely the displacement of the cylinder) and the angle of crank θ (namely the pitch angle β) can be expressed:

$$y = r(1-\cos\theta) + l[1 - \sqrt{1 - (\frac{r}{l}\sin\theta)^2}\,] \quad (18)$$

where l is the distance from A to B (mm), r is the distance from B to C (mm).

3 Control Strategies

The conventional PID controller output $u(t)$ is given by expression

$$u(t) = k_P\left\{e(t) + \frac{1}{T_I}\int_0^t e(\tau)d\tau + T_D\frac{de(t)}{dt}\right\}$$
$$= k_P e(t) + k_I\int_0^t e(\tau)d\tau + k_D\frac{de(t)}{dt} \quad (19)$$

where $e(t)$ is the error input, T_I is the integral time constant, T_D is the derivative time constant, k_P is the proportional gain, $k_I = k_P / T_I$ is the integral gain, $k_D = k_P T_D$ is the derivative gain. The role of each separate part of a PID controller can be described as follows: The proportional part reduces the error responses of the system to disturbances, the integral part eliminates the steady-state error of the system, and the derivative part dampens the dynamic response and thereby improves the stability of the system. From the perspective of time, the proportional part estimates the system at present, the integral part takes the past into account, and the derivative part estimates what will happen in the future, which yields a much more stable control than the control with only one or two of these features [12]. The fuzzy controller may adjust on-line the proportional, integral and derivative gain of a conventional PID controller according to value of input $e(t)$. These gains are expressed as:

$$k_P = k_P^* + \Delta k_P \cdot k_{\Delta k_P} \tag{20}$$

$$k_I = k_I^* + \Delta k_I \cdot k_{\Delta k_I} \tag{21}$$

$$k_D = k_D^* + \Delta k_D \cdot k_{\Delta k_D} \tag{22}$$

where k_P^*, k_I^*, k_D^* are initial values, Δk_P, Δk_I, Δk_D are given by expression

$$\Delta k_P = \{e \times \dot{e}\} \circ R_{\Delta k_P} \tag{23}$$

$$\Delta k_I = \{e \times \dot{e}\} \circ R_{\Delta k_I} \tag{24}$$

$$\Delta k_D = \{e \times \dot{e}\} \circ R_{\Delta k_D} \tag{25}$$

where $R_{\Delta k_P}$, $R_{\Delta k_I}$, $R_{\Delta k_D}$ are fuzzy decision relation matrixes. The fuzzy rules and membership functions have been designed to optimize the captured power at low wind speed and to limit the captured power at high wind speed [13, 14]. The two inputs are the DFIG rotor angular velocity error and its differential error at variable speed control, the fundamental universe of error is [-4000, 4000], the fundamental universe of differential error is [-50000, 50000], and the fundamental universe of control variable is [-250, 250]. The two inputs are the DFIG power error and its differential error at variable pitch control, the fundamental universe of error is [-60000, 60000], the fundamental universe of differential error is [-300000, 300000], and the fundamental universe of control variable is [-13, 13]. The fuzzy controller adopts the triangle function, the Mamdani MaxMin fuzzy reasoning and the Maxsubjection degree method. The fuzzy universe is [-1 -0.8 -0.6 -0.4 -0.2 0 0.2 0.4 0.6 0.8 1], as shown in Fig.4. The rules of the AFPIDC modification gain Δk_P, Δk_I, Δk_D are produced based on the rules summarized in Table 1, Table 2, Table 3.

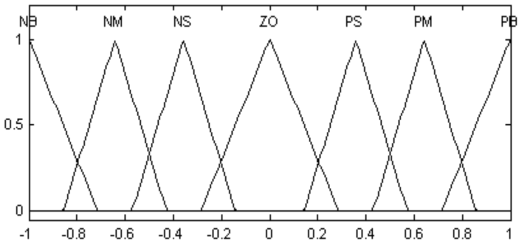

Fig.4 Membership functions for input and output variables

Table 1
Rules for Proportional Modification Gain

Δk_P \ $\dot{e}$ / e	NB	NM	NS	ZO	PS	PM	PB
NB					PM	PS	ZO
NM		PB		PM	PS	ZO	NS
NS			PM	PS	ZO	NS	NM
ZO		PM	PS	ZO	NS	NM	
PS	PM	PS	ZO	NS	NM		
PM	PS	ZO	NS	NM		NB	
PB	ZO	NS	NM				

Table 2
Rules for Integral Modification Gain

Δk_I \ $\dot{e}$ / e	NB	NM	NS	ZO	PS	PM	PB
NB			ZO		NS	ZO	ZO
NM				NS	NS	ZO	ZO
NS	NS	NM	NS	NS	ZO	PS	PM
ZO	NB	NM	NS	ZO	PS	PM	PB
PS	NM	NS	ZO	PS	PS	PM	PS
PM	ZO	ZO	PS	PS		ZO	
PB	ZO	ZO	PS				

Table 3
Rules for Derivative Modification Gain

Δk_D \ $\dot{e}$ / e	NB	NM	NS	ZO	PS	PM	PB
NB	PS	NM	NB	NB	NB	NM	PS
NM	PS	NS	NB	NM	NM	NS	PS
NS	ZO	NS	NM	NS	NS	NS	ZO
ZO	ZO	NS	NS	NS	NS	NS	ZO
PS	ZO	ZO	ZO	ZO	ZO	ZO	ZO
PM	PM	PS	PS	PS	PS	PS	PB
PB	PB	PM	PM	PM	PS	PS	PB

Each input and output variable has its own control surface, which consists of fuzzy region. These regions overlap each other to give a smooth control response. The area in which membership functions are dense is where accurate control is crucial. The input and output regions are related by a set of rules. Once the fuzzy controller is activated, rule evaluation is performed and all the rules that are true are fired. The rules and membership functions have been designed and adjusted based on simulations, testing and knowledge of the characteristics and response for the wind turbine system. Where: P means positive, N means negative, B means big and S means small.

4 Simulation

Simulation study is done for a 1.5 MW wind generation system with the simulation software MATLAB/SIMULINK. A ramp response simulation has been performed to evaluate the behaviour of the controller. There is no turbulence, tower shadow or wind shear [15]. Wind turbine start to provide power from 4 m/s wind speed (cut-in wind speed). Maximum power is nearly given for 12.2 m/s wind speed (rated wind speed). Wind speed higher than 25 m/s (cut-out wind speed) is recommended to brake wind turbine. The following system parameters are obtained from real product samples.

A. Rotor speed range: 11.1-22.2 r/min, Diameter =70.5 m, Cut in wind speed=4 m/s, Rated wind speed=12.2 m/s, Cut out wind speed=25 m/s, Gearbox ratio=1: 90, Optimum tip speed ratio=10, Optimum power coefficient=0.44, Turbine rotor inertia=320000 kg·m^2.

B. Generator pole=4, Rated power=1.5 MW, Rated frequency=50 Hz, Stator rated voltage=690 V, Rotor rated voltage=690 V, Stator resistance (pu)=0.0076, Rotor resistance (pu)=0.0073, Stator leakage inductance (pu)=0.1248, Rotor leakage inductance (pu)=0.0884, Magnetizing inductance (pu)=1.8365, Generator rotor inertia=60 kg·m^2, Power factor =1.

C. K_i=0.3 N/mA, K_c=0.026×10^{-10} m^5/N·s, M=5000 kg, β_e=7000×10^5 N/m^2, A_c=12.7 cm^2, K_{sf}=8.4 N·m/rad, K_a=0.356 m^2/s, V_c=8.38×10^{-4} m^3, K_s=0.4 mA/mm, r=480 mm, l=600 mm.

When the wind speed range varies from 4 to 12.2 m/s, AFPID-VS control method is adopted by adjusting the rotor speed in order to obtain the optimal value of λ. So, through changing the tip speed ration induced by rotor speed or wind speed, can leading to get the optimal power coefficient $C_{p-opt}(\lambda,\beta)$, namely obtain the maximum power by adjusting value of λ. As shown in Fig.2, $C_{p-opt}(\lambda,\beta)$ is about 0.44, where $\lambda=10$, $\beta=0$. When the wind speed range varies from 12.2 to 25 m/s, AFPID-VP control method is adopted by adjusting the pitch angle β in order to make generator work in the case of rated power.

Fig.5 shows the ramp wind speed changes with the time from 0 to 21 s. Fig.6 shows the $C_{p-opt}(\lambda,\beta)$ changes in AFPID-VS control and its value equals to 0.44 approximately. Fig.7 shows the $C_p(\lambda,\beta)$ changes in AFPID-VP control, and Fig.8 also shows the pitch angle β changes. It can be seen that the $C_p(\lambda,\beta)$ changes small as the pitch angle β changes big. Fig.9 shows the DFIG rotor control current changes in AFPID-VS control, and Fig.10 shows the control current of the electro-hydraulic proportional valve changes in AFPID-VP control. It is obvious that the control current of the electro-hydraulic proportional valve is proportional to the wind speed.

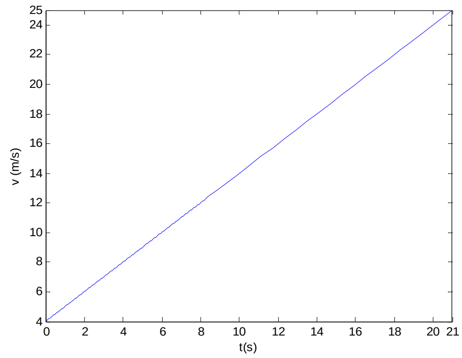

Fig.5 Wind speed changing in AFPID control

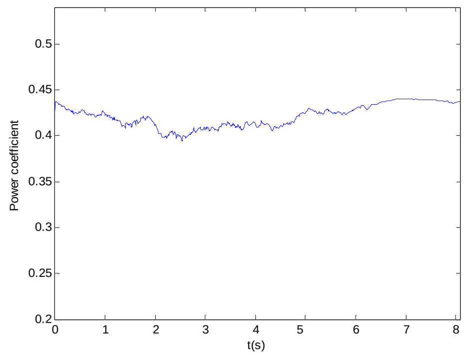

Fig.6 $C_{p-opt}(\lambda,\beta)$ changing in AFPID-VS control

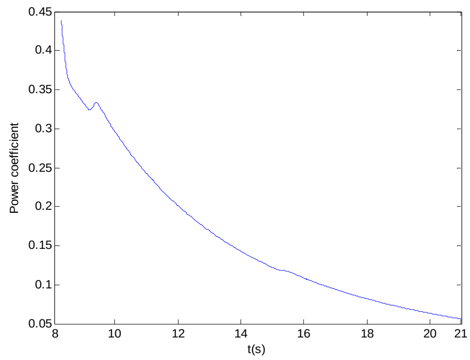

Fig.7 $C_p(\lambda,\beta)$ changing in AFPID-VP control

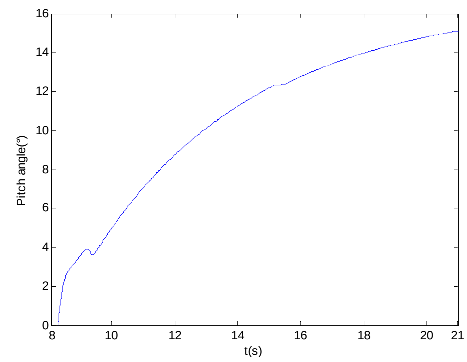

Fig.8 Pitch angle changing in AFPID-VP control

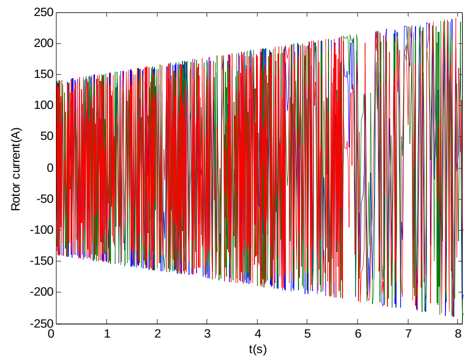

Fig.9 DFIG rotor control current changing in AFPID-VS control

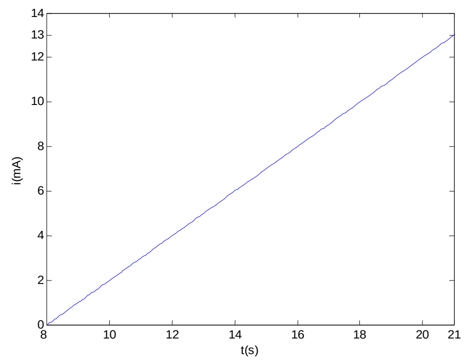

Fig.10 Control current of the electro-hydraulic proportional valve in AFPID-VP control

Fig.11 shows the DFIG rotor speed changes with the wind speed from 4 to 25 m/s. It can be seen that the rotor speed changes in order to get a $C_{p-opt}(\lambda,\beta)$ in AFPID-VS control, but the rotor speed maintains rated value 2000 rpm in AFPID-VP control. Fig.12 shows the DFIG power changes with the wind speed from 4 to 25 m/s. It is obvious that the AFPID control strategy has the optimal performance than the conventional PID control strategy. We may obtain the maximum power in AFPID-VS control and the rated power in AFPID-VP control.

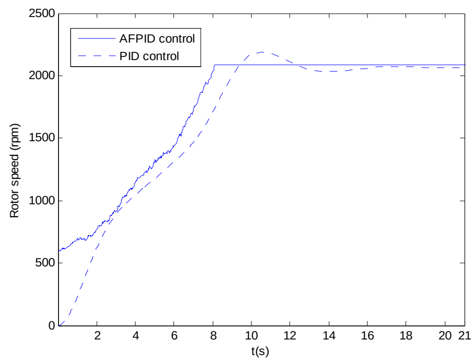

Fig.11 DFIG rotor speed changing in AFPID control

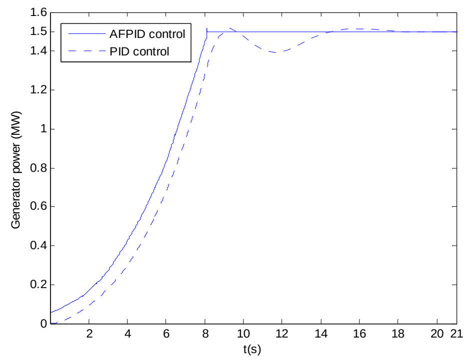

Fig.12 DFIG power changing in AFPID control

5 Conclusion

The paper presents a dynamic model for a 1.5 MW VS-VP wind generation system with the DFIG and the HVPM. When the wind speed range varies from the cut-in wind speed to the rated wind speed, the AFPID-VS control method is adopted by adjusting the rotor speed in order to obtain the maximum power. When the wind speed range varies from the rated wind speed to the cut-out wind speed, the AFPID-VP control method is adopted by adjusting the pitch angle in order to make generator work in the case of the rated power.

Simulation results show the AFPIDC can shorten the system response times, compensate the system nonlinearity and eliminate the steady state error due to uncertain factor and external disturbances, and improve the wind generation system performance at low, rated and high wind speed.

References:

[1] Simoes M.G., Bose B.K., Spiegel R.J, Design and Performance Evaluation of A Fuzzy-logic-Based Variable-Speed Wind Generation System, *IEEE Transactions on Industry Application*, Vol.33, No.4, 1997, pp. 956-965.

[2] F. Blaabjerg, Z. Chen, R. Teodorescu, F. Iov, Power Electronics in Wind Turbine Systems,

CES/IEEE 5th international power electronics and motion control conference, Vol.1, No.5, 2006, pp. 46-57.

[3] Camblong H., Vidal M. Rodriguez, Puiggali J.R., Principles of A Simulation Model for A Variable-Speed Pitch-Regulated Wind Tturbine, *Wind Engineering*, Vol.28, No.2, 2004, pp. 157-175.

[4] Prats M.M., Carrasco J.M., Galvan E., Sanchez J.A., Franquelo L.G, A New Fuzzy Logic Controller to Improve the Captured Wind Energy in A Real 800 kW Variable Speed-Variable Pitch Wind Turbine, *Power Electronics Specialists Conference, IEEE 33rd Annual*, Vol.1, No.23, 2002, pp. 101 -105.

[5] Perales M., Perez J., Barrero F., Mora J.L., Galvan, E., Carrasco J.M., Franquelo L.g., de la Cruz D., Fernandez L., Zazo A.L., Fuzzy Logic Control of A Variable Speed, Variable Pitch Wind Turbine, *Industrial Electronics Society, The 25th Annual Conference of the IEEE*, Vol.2, No.29, 1999, pp. 614-618.

[6] Simoes M.G., Bose B.K., Spiegel R.J., Fuzzy Logic Based Intelligent Control of A Variable Speed Cage Machine Wind Generation System, *Power Electronics Specialists Conference, 26th Annual IEEE*, Vol.1, No.18, 1995, pp. 389-395.

[7] Yifan Tang, Longya Xu, Adaptive Fuzzy Control of A Variable Speed Power Generating System with Doubly Excited Reluctance Machine, *Power Electronics Specialists Conference, 25th Annual IEEE*, Vol.1, 1994, pp. 377-384.

[8] Wu Li, Wang Zhixin, Junji Tamura, Smoothing Control of Wind Farm Output Fluctuation with Doubly-fed Asynchronous Machine, *Proceeding of IEEE PEDS*, 2005, pp.495-500.

[9] Hansen A.D., Sørensen P., Lov F., Blaabjerg F, Control of Variable Speed Wind Turbines with Doubly-fed Induction Generators, *Wind Engineering*, Vol.28, No.4, 2004, pp. 411-432.

[10] Rogério G de Almeida, J A Peças Lopes, J A L Barreiros, Improving Power System Dynamic Behavior Through Doubly Fed Induction Machines Controlled by Static Converter Using Fuzzy Control, *IEEE Transactions on Power Systems*, Vol.19, No.3, 2004, pp. 1942-1950.

[11] Z. Shi, F. Gu, B. Lennox, A.D. Ball, The Development of An Adaptive Threshold for Model-Based Fault Detection of A Nonlinear Electro-Hydraulic System, *Control Engineering Practice*, Vol.13, No.11, 2005, pp. 1357-1367.

[12] Tan Guan-zheng, Zeng Qing-dong, He Sheng-jun, Adaptive and Robust Design for PID Controller Based on Ant System Algorithm, *Advances in Natural Computation Lecture Notes in Computer Science*, Vol.36, No.5, 2005, pp. 915-924.

[13] Abo-Khalil A.G., Dong-Choon Lee, Jul-Ki Seok, Variable Speed Wind Power Generation System Based on Fuzzy Logic Control for Maximum Output Power Tracking, *Power Electronics Specialists Conference,IEEE 35th Annual*, Vol.3, No.20-25, 2004, pp. 2039-2043.

[14] Prats M.M., Carrasco J.M., Galvan E., Sanchez J.A., Franquelo L.G., Batista C., Improving Transition Between Power Optimization and Power Limitation of Variable Speed, Variable Pitch Wind Turbines Using Fuzzy Control Techniques, *Industrial Electronics Society, 26th Annual Conference of the IEEE*, Vol.3, No.22, 2000, pp. 1497-1502.

[15] Hansen M.H., Hansen Anca, Larsen T.J., Øye Stig, Sørensen P., Fugisang Pete, *Control Design for A Pitch-Regulated, Variable Speed Wind Turbine*, Risø National Laboratory, 2005.